

PARAMETER ESTIMATION OF MULTICOMPONENT QUADRATIC FM SIGNALS USING COMPUTATIONALLY EFFICIENT RADON-CPF TRANSFORM

Pu Wang and Jianyu Yang

School of Electronic Engineering, University of Electronic Science and Technology of China
No.4, Sect.2, North Jianshe Road, 610054, Chengdu, P.R.China
phone: + (86) 8320 4368, fax: + (86) 8320 1448, email: pwang@ieee.org

ABSTRACT

The identifiability problem of the cubic phase function (CPF) for multicomponent quadratic FM (QFM) signals is verified both in theory and in simulations. A computationally efficient technique based on the one dimensional (1-D) Radon-CPF transform (RCT) is proposed for this problem. The RCT first reassigns the time-frequency rate distribution (TFRD) with the information of the second-order coefficient, and then implements the 1-D Radon transform with only angle variety. Although this technique is supposed for multicomponent QFM signals, it is also efficient for monocomponent. The simulation results verify the proposed method both in illustrative examples and performance evaluations.

1. INTRODUCTION

The frequency-modulated (FM) signals are usually used in numerous areas, such as communication, radar, biomedicine, and seismic analysis. This paper focuses the analysis on the quadratic FM (QFM) signals. Two practical applications of this kind of signal can be found in [1, 2]. The first application is the passive intelligent radar surveillance, where one tries to determine whether a linear FM, QFM, or other type of radar pulse is being transmitted. The other application is in the processing of echolocation signals from brown bats. These signals are multicomponent QFM sonar signals, with the parameters of the FM signals varying according to the activity of the bat.

In the literature, the Maximum likelihood (ML) estimation is efficient to estimate the parameters of the QFM signal. The direct implementation, however, requires three-dimensional (3-D) maximization. Moreover, if the objective function is not convex, ML estimation is likely to converge to local maxima. To avoid the exhaustive 3-D grid search, the suboptimal techniques are developed, such as the phase unwrapping [3], the polynomial phase transform (PPT) [4], the product high-order ambiguity function (PHAF) [5], and the method based on stationary high-order moments [6]. The main shortcoming of these methods is the poor performance at low SNR, i.e., below 0 dB, since they employ highly nonlinear transform. To improve the performance at low SNR, P. O'Shea proposed a bilinear transform, which is known as cubic phase function (CPF) or time-frequency rate distribution (TFRD) [2, 7] for parameter estimation of a QFM signal with only second-order nonlinearity. For multi-

component QFM signals, the spurious peaks arise and thus the identifiability problem occurs. In [8], the product CPF (PCPF) is proposed to analyze the multicomponent linear FM signals. The extension for multicomponent QFM signal, however, has not yet been implemented.

In this paper, we consider the combination of the CPF and Radon transform for elimination of the identifiability problem. Since the direct combination of two techniques result in two-dimensional (2-D) maximization and corresponding 2-D grid search, a computationally efficient Radon-CPF transform (RCT) is proposed. The RCT utilizes the second-order coefficient to reassign the TFRD for implementation of the Radon transform with only one parameter of the rotation angle. Specifically, two forms of the 1-D/2-D RCT are discussed: the envelope estimator and the modulus square estimator.

The paper is organized as follows. In section 2, the definition of the CPF and the problem formulation are described. Section 3 first defines the 2-D RCT, and then proposes the 1-D RCT for multicomponent QFM signals. The computation complexity and the constraint are also discussed. Section 4 provides illustrative examples and performances in the both case of the 1-D/2-D RCT. Finally, conclusion is drawn in Section 5.

2. CUBIC PHASE FUNCTION AND PROBLEM FORMULATION

2.1 Cubic Phase Function

The CPF is defined as a 2-D bilinear transform efficient for estimating the instantaneous frequency rate (IFR) [7]. The estimated IFR is used as an initial step in estimating other phase parameters. The IFR of a signal $s(n)$ with phase $\phi(n)$ is defined as

$$\text{IFR}(n) = d^2\phi(n)/dn^2. \quad (1)$$

The discrete CPF for a signal $s(n)$ is given by

$$\text{CPF}(n, \Omega) = \int_0^{+\infty} x(n+\tau)x(n-\tau)e^{-j\Omega\tau^2} d\tau, \quad (2)$$

where Ω represents the IFR. For a QFM signal as

$$s(n) = Ae^{j(a_0+a_1n+a_2n^2+a_3n^3)}, \quad n \in \psi \quad (3)$$

where $\psi = [-(N-1)/2 : (N-1)/2]$, N is odd, the CPF results in

$$CPF(n, \Omega) = A^2 \xi(n) \int_0^{+\infty} e^{j[(2a_2 + 6a_3n) - \Omega] \tau^2} d\tau \quad (11)$$

$$= \begin{cases} A^2 \xi(n) \sqrt{\frac{\pi}{8|(2a_2 + 6a_3n) - \Omega|}} (1 + j), & (2a_2 + 6a_3n) > \Omega \\ A^2 \xi(n) \sqrt{\frac{\pi}{8|(2a_2 + 6a_3n) - \Omega|}} (1 - j), & (2a_2 + 6a_3n) < \Omega \end{cases} \quad (4)$$

where $\xi(n) = e^{j2(a_0 + a_1n + a_2n^2 + a_3n^3)}$. Obviously, the CPF achieves maxima along the IFR $\Omega = 2a_2 + 6a_3n$. By exploiting the dependence of IFR on time, the algorithm in [7] estimates phase parameters using two slices of CPF. The selection of the time positions are also analysis: $n = 0$ is used to reduce the variance of a_3 and a_2 and $n \approx 0.11N$ is used to lower the mean-square error (MSE) of a_3 .

2.2 Problem Formulation

The CPF has good performance and computational implementation for monocomponent QFM signal at low SNR [2]. For multicomponent QFM signals, however, the CPF fails to estimate phase parameters at the time positions where the spurious peaks are presented. In [8], for multicomponent linear FM signals, the authors utilized the different time dependences of the auto terms and spurious peaks in TFRD to efficiently solve the identifiability problem. The direct extension for QFM signals, however, is not able to discern the auto terms and cross terms, since both of auto terms and cross terms occur along a function of the time.

To formulate the identifiability problem, consider two QFM signals:

$$x(n) = A_1 e^{j(a_{1,0} + a_{1,1}n + a_{1,2}n^2 + a_{1,3}n^3)} + A_2 e^{j(a_{2,0} + a_{2,1}n + a_{2,2}n^2 + a_{2,3}n^3)} \quad (5)$$

Substituting (5) into (1), the $x(n + \tau)x(n - \tau)$ has four items: two auto terms and two cross terms. The results of auto terms are:

$$A_i^2 e^{j(2a_{i,0} + 2a_{i,1}n + 2a_{i,2}n^2 + 2a_{i,3}n^3)} e^{j(2a_{i,2} + 6a_{i,3}n)\tau^2}, \quad i = 1, 2. \quad (6)$$

From (6), each auto term occurs along respective IFR as $\Omega = 2a_{i,2} + 6a_{i,3}n$. In contrast, the cross terms are derived as:

$$\begin{cases} A_1 A_2 z(n) e^{j[(a_{1,1} - a_{2,1}) + 2(a_{1,2} - a_{2,2})n + 3(a_{1,3} - a_{2,3})n^2] \tau + [(a_{1,2} + a_{2,2}) + 3(a_{1,3} + a_{2,3})n] \tau^2 + (a_{1,3} - a_{2,3}) \tau^3} \\ A_1 A_2 z(n) e^{j[(a_{2,1} - a_{1,1}) + 2(a_{2,2} - a_{1,2})n + 3(a_{2,3} - a_{1,3})n^2] \tau + [(a_{1,2} + a_{2,2}) + 3(a_{1,3} + a_{2,3})n] \tau^2 + (a_{2,3} - a_{1,3}) \tau^3} \end{cases} \quad (7)$$

where $z(n) = e^{j[(a_{1,0} + a_{2,0}) + (a_{1,1} + a_{2,1})n + (a_{1,2} + a_{2,2})n^2 + (a_{1,3} + a_{2,3})n^3]}$. From (7), the troublesome cross terms occurs along a nonlinear function of the time. In particular, if

$$\begin{cases} (a_{1,1} - a_{2,1}) + 2(a_{1,2} - a_{2,2})n = 0, \\ a_{1,3} - a_{2,3} = 0 \end{cases}, \quad (8)$$

the two cross terms merge into one item as

$$A_1 A_2 z(n) e^{j[(a_{1,2} + a_{2,2}) + 3(a_{1,3} + a_{2,3})n] \tau^2}, \quad (9)$$

In this case, the spurious peak arise at $\Omega = (a_{1,2} + a_{2,2}) + 3(a_{1,3} + a_{2,3})n$, where n is subject to (8). Indeed, only if

$$(a_{1,1} - a_{2,1}) + 2(a_{1,2} - a_{2,2})n + 3(a_{1,3} - a_{2,3})n^2 = 0, \quad (10)$$

The cross terms reduce to

respectively.

Note that to avoid ambiguities inherent in the phase parameters, it is assumed that $|a_1| \leq \pi$, $|a_2| \leq \pi/N$, $|a_3| \leq 3\pi/2N^2$. Therefore, the phase in (11) is dominated by the term as $[(a_{1,2} + a_{2,2}) + 3(a_{1,3} + a_{2,3})n] \tau^2$, since the term as $(a_{2,3} - a_{1,3}) \tau^3$ is too small with respected to $[(a_{1,2} + a_{2,2}) + 3(a_{1,3} + a_{2,3})n] \tau^2$. The equation (11), hence, can be approximately rewritten into one term as

$$A_1 A_2 z(n) e^{j[(a_{1,2} + a_{2,2}) + 3(a_{1,3} + a_{2,3})n] \tau^2}, \quad (12)$$

which presents the spurious peaks around $\Omega \approx (a_{1,2} + a_{2,2}) + 3(a_{1,3} + a_{2,3})n$, where n is subject to (10). Note that the spurious peaks are generally diffused due to the phase approximation. The illustration is drawn in *Example 1*.

3. THE COMPUTATIONALLY EFFICIENT RADON-CPF TRANSFORM

As indicated above, the CPF is not able to analyze the multicomponent QFM signals due to the arising of the spurious peaks. This identifiability problem should be removed for the purpose of detection and parameter estimation. The direct combination of the Radon transform and the CPF is first proposed to solve this problem. However, the limitation of this technique is the computation burden with 2-D maximization and its resulting 2-D grid search. In this session, we proposed a computationally improved RCT with the aim to fast implementation and good performance at low SNR. The novel Radon-CPF is to first estimate the IFR at $n = 0$, which is equal to twice of the second-order coefficient a_2 , then reassign the CPF with the estimated second-order coefficient, and finally implement the Radon transform to extract the corresponding signal.

3.1 The Radon transform

The Radon transform in [10], which is commonly used in image signal processing, also has various applications in the area of signal detection and estimation. Its definition is:

$$R_{s,\theta} = \int_{-\infty}^{+\infty} \int_{-\infty}^{+\infty} f(x, y) \delta(x \sin \theta + y \cos \theta - s) dx dy, \quad (13)$$

for $-\infty < s < +\infty$ and $0 \leq \theta < \pi$, where the delta function specifies the direction of integration. The parameter s and θ represent the angle with the x axis and shifted location of the origin, respectively. Two typical applications of Radon transform in detection and parameter estimation are the Radon-Wigner transform (RWT) [9] and the Radon-Ambiguity transform (RAT) [10].

3.2 The 2-D Radon-CPF transform

In this subsection, we briefly define the RCT. The direct combination of Radon transform and the CPF results in the 2-D RCT. In particular, two forms of the 2-D Radon CPF transform are defined as follow:

Envelope estimator:

$$\begin{aligned}
 R_{s,\theta} &= \int_{-\infty}^{+\infty} \int_{-\infty}^{+\infty} |CPF(n, \Omega)| \delta(n \sin \theta + \Omega \cos \theta - s) dn d\Omega \\
 &= \int_{-\infty}^{+\infty} |CPF(n, \Omega_0 - kn)| dn
 \end{aligned} \tag{14}$$

Modulus square estimator:

$$\begin{aligned}
 R'_{s,\theta} &= \int_{-\infty}^{+\infty} \int_{-\infty}^{+\infty} |CPF(n, \Omega)|^2 \delta(n \sin \theta + \Omega \cos \theta - s) dn d\Omega \\
 &= \int_{-\infty}^{+\infty} |CPF(n, \Omega_0 - kn)|^2 dn
 \end{aligned} \tag{15}$$

where Ω_0 and k are the initial IFR and the change of IFR, respectively. For a given k , the integral corresponds to a slice through $R_{s,\theta}$ and $R'_{s,\theta}$ at angle $\theta = \arctan(-1/k)$ with the projection axis, s , scaled by $1/\sin(\theta)$. If the direction coincides with the IFR, the integral sums up all energy of auto terms and present a distinct peak. According to this, the parameter estimation can be achieved by

$$\begin{cases} \hat{a}_2 = s/2 \sin(\theta) \\ \hat{a}_3 = -\cot(\theta)/6 \end{cases} \tag{16}$$

On the other hand, it is obvious that both of (14) and (15) are the 2-D transform and require corresponding 2-D grid search, which is not easily for fast implementation.

3.3 The 1-D Radon-CPF transform

3.3.1 The 1-D Radon-CPF Transform

In order to reduce the computation and exhaustive 2-D grid search, a computationally efficient RCT is proposed in this subsection. The motivation behind this idea is that the computationally efficient RAT only integrals the straight line across the origin in the ambiguity function. The computation thus can be reduced if we can reassign the CPF and only integral the straight line across the origin in the TFRD.

The question in the reassign operation is how to appropriately adjust the CPF. The obvious approach is to first estimate the second-order coefficient a_2 and move the CPF down or up along the IFR axis based on the distance from a_2 to the origin. Mathematically, this operation can be described as:

$$\Omega_{shift} = 2a_2, \tag{17}$$

and

$$CPF_{shift}(n, \Omega') = CPF(n, \Omega - \Omega_{shift}). \tag{18}$$

Substituting (4) into (18), yields,

$$|CPF_{shift}(n, \Omega')| = A^2 \sqrt{\frac{\pi}{4|6a_3n - \Omega'|}}. \tag{19}$$

Once the reassign operation is finished, the auto terms distribute along the straight line across the origin in the TFR domain. Note that each reassign operation only makes one component pass through the origin in the TFR domain. Then the third-order coefficient can be estimated by a 1-D grid search over the Radon transform domain:

Envelope estimator:

$$\begin{aligned}
 R_{shift}(k) &= \int_{-\infty}^{+\infty} \int_{-\infty}^{+\infty} |CPF_{shift}(n, \Omega')| \delta(n \sin \theta + \Omega' \cos \theta - s) dn d\Omega' \Big|_{s=0}
 \end{aligned}$$

$$\begin{aligned}
 &= \int_{-\infty}^{+\infty} \int_{-\infty}^{+\infty} |CPF_{shift}(n, \Omega')| \delta(\Omega' - kn) dn d\Omega' \Big|_{k=-\cot(\theta)} \\
 &= \int_{-\infty}^{+\infty} |CPF_{shift}(n, kn)| dn
 \end{aligned} \tag{20}$$

Modulus square estimator:

$$R'_{shift}(k) = \int_{-\infty}^{+\infty} |CPF_{shift}(n, kn)|^2 dn \tag{21}$$

Substituting (19) into (20) and (21), in addition to $n \in \psi$, the results of the 1-D Radon transform can be derived as

$$R_{shift}(k) = A^2 \sqrt{\frac{\pi(N-1)}{8|6a_3 - k|}} \tag{22}$$

and

$$R'_{shift}(k) = \frac{\pi A^4 \ln[(N-1)/2]}{2|6a_3 - k|} \tag{23}$$

From (22) and (23), both estimators achieve maxima at the angle as $\text{arccot}(-6a_3)$, while presenting finite energy at other angles.

3.3.2 Separation of multicomponent quadratic FM signals

For multicomponent QFM signals, the RCT sequential extract one signal once, which is different from the case of the 2-D RCT simultaneously employs the integral over all the components. Therefore, the 1-D RCT introduces much less cross terms and noise into the Radon transform domain.

Moreover, the 1-D RCT also has ability to resolve closely-spaced QFM signals, since both of the reassign operation and the Radon transform can be used to distinguish two signals. In specific, the algorithm in [2], with a coarse estimation and subsequent refined estimation, is able to first discern two closely-spaced second-order coefficients. Based on it, the reassign operation just makes the auto terms of one signal occur across the origin in the TFRD. Once the first step finishes, the Radon transform with small variety of the rotational angle is utilized for further signal separation, especially the signals with closely-spaced third-order coefficients.

3.3.3 Computational complexity

We first list the computations in the 2-D RCT: the fast computation of the CPF with subband decomposition [2], 2-D Radon transform over the CPF, and 2-D grid search in the Radon transform domain. In contrast, the 1-D RCT requires: the fast computation of the CPF, a 1-D grid search in the CPF at $n=0$, reassign operation, 1-D Radon transform over the CPF, and a 1-D grid search. The computation reduces mainly due to much less integrals and grid search.

Within other techniques for multicomponent QFM signals, the PPT and the PHAF with small lag sets are faster than the RCT; the Radon-Wigner transform (RWT) suffers from 2-D grid search; The integrated general ambiguity function (IGAF) [11] is also computationally exhaust.

In conclusion, the 1-D RCT can be treated as, in addition to good performance at low SNR and suppression of spurious peaks, one of the computationally efficient transform for multicomponent QFM signals.

3.3.4 Constraint

The 1-D RCT has the constraint on estimating the second-order coefficient in assign operation. From (8) and (10), if the spurious peaks arise at $n=0$, the first-order coefficients must be same. Therefore, we make the assumption that the first-order coefficients of all signals are distinct which results in the spurious peaks occur at $n \neq 0$.

4. SIMULATIONS

In this section, we first demonstrate the identifiability problem, then the direct illustration and finally the performance of the 1-D/2-D RCT with respect to the Cramér-Rao lower Bound (CRLB). Due to the proposed algorithm is sequential, it inevitably suffers from error propagation effect. Therefore, only the MSEs of the third-order coefficient are evaluated.

Example 1 – To demonstrate the identifiability problem and the illustration of the 1-D/2-D Radon-CPF transform.

Two signals are generated by (3) and the parameters are chosen to be $A_1=1$, $a_{1,0}=0$, $a_{1,1}=\pi/25$, $a_{1,2}=\pi/5N$, $a_{1,3}=\pi/5N^2$, and $A_2=1$, $a_{2,0}=0$, $a_{2,1}=-\pi/25$, $a_{2,2}=-\pi/10N$, $a_{2,3}=\pi/5N^2$ (fig.1 (a)) or $a_{2,3}=2\pi/5N^2$ (fig.1 (b)), respectively. $N=515$ and the sampling rate is 1.

The simulation results of *example 1* are plotted in Fig.1. The identifiability problem is easy to see from Fig.1 (a-b). The results of the 1-D RCT are indicated with plus signs, whereas the results of the 2-D RCT are shown as circles. Note that the results of the 2-D Radon-CPF are plotted at the slice where the distinct peaks occur. From Fig. 1, it is evident that the 1-D RCT has similar performance for multi-component QFM signals.

Examples 2 – To evaluate the performance of the 1-D/2-D Radon-CPF transform. Due to the error propagation effect, only the third-order coefficient is considered. The simulation results show other phase estimations have similar performance, i.e., the SNR threshold, as well. In order to compare with other algorithms, especially the PPT and CPF, the same signal in [2, 12] is used with parameter as, $a_0=0$, $a_1=0.3\pi$, $a_2=-\pi 10^{-3}$, $a_3=\pi 10^{-5}$, $N=257$ and sampling rate is 1. The MSEs of estimates are evaluated as

$$\text{MSE}_{a_3} = \sum_{i=1}^M |a_3 - \hat{a}_3|^2 / M . \quad (24)$$

where $M=250$ is the Monte-Carlo runs for each SNR. The SNR is varied from -10 dB to 10 dB by a step of 1 dB.

The measured MSEs are plotted in Fig.2. Both cases of the 1-D and 2-D RCT are evaluated. For high input SNR, the envelop form of the 1-D transform has an about 1.32 dB loss compared with the CRLB, whereas the square-law estimator has an about 2 dB loss results for its higher order of nonlinearity. For the comparison, the corresponding performances loss of envelope form and square-law form of the 2-D RCT are shown about 4 dB and 6 dB, respectively. For lower SNR, the performances of all estimators degrade dramatically.

From Fig. 2, it is evident that the 1-D RCT has the SNR threshold at -3 dB, whereas the SNR threshold of the 2-D

RCT is about 5 dB. In [2] and [12], the CPF and PPT are shown to threshold at higher SNR, i.e., -2 dB and 6 dB, respectively.

5. CONCLUSION

A computationally efficient technique has been proposed for elimination of the identifiability problem arising from multi-component QFM signals. This technique utilizes the second-order coefficient to reassign the TFRD with the aim to implement only angle integrals. Once the reassign operation is finished, the multicomponent case can be expressed sequential monocomponent cases, which introduces much less cross terms in the Radon transform domain. In numerical simulations, the performances of the 1-D and 2-D RCT are evaluated. Compared with other techniques for multicomponent QFM signals, the 1-D Radon transform can be considered as the good trade-off between the computation complexity and the performance.

REFERENCES

- [1] S. Peleg and B. Friedlander, "Multicomponent signal analysis using the polynomial phase transform", *IEEE Trans. Aerosp. Electron. Syst.*, vol. 32, pp. 378-386, Jan. 1996.
- [2] P. O'Shea, "A fast algorithm for estimating the parameters of a quadratic FM Signal," *IEEE Trans. Signal Process.*, vol. 52, pp. 385-393, Feb. 2004.
- [3] P.M. Djuric and S.M. Kay, "Parameter estimation of chirp signals," *IEEE Trans. Signal Process.*, vol. 38, pp. 2118-2126, Dec. 1990.
- [4] S. Peleg and B. Friedlander, "The discrete polynomial phase transform," *IEEE Trans. Signal Process.*, vol. 43, pp. 1901-1914, Aug. 1995.
- [5] S. Barbarossa, A. Scaglione, and G B. Giannakis, "Product high-order ambiguity function for multicomponent polynomial-phase signal modelling," *IEEE Trans. Signal Process.*, vol. 46, pp. 691-708, March 1998.
- [6] A. Ferrari, C. Theys, and G. Alengrin, "Polynomial phase signal analysis using stationary moments," *Signal Process.*, vol. 54, pp. 239-248, 1996.
- [7] P. O'Shea, "A new technique for estimating instantaneous frequency rate," *IEEE Signal Process. Lett.*, vol. 9, pp. 251-252, Aug. 2002.
- [8] P. Wang, J. Yang and J. Xiong, "An algorithm for parameter estimation of multicomponent chirp signals," in *Proc. ICASSP 2006*, Toulouse, France, May 14-19, 2006.
- [9] S. Barbarossa, "Analysis of multicomponent LFM signals by a combined Wigner-Hough transform," *IEEE Trans. Signal Process.*, vol. 43, pp. 1511-1515, June 1995.
- [10] M. Wang, A. K. Chan and C. K. Chui, "Linear frequency-modulated signal detection using Radon-Ambiguity transform," *IEEE Trans. Signal Process.*, vol. 46, pp. 571-586, March 1998.
- [11] S. Barbarossa and V. Petrone, "Analysis of polynomial-phase signals by the integrated generalized ambiguity function," *IEEE Trans. Signal Process.*, vol. 45, pp. 316-327, Feb. 1997.

[12] S. Peleg and B. Friedlander, "The discrete polynomial phase transform," *IEEE Trans. Signal Process.*, vol. 43, pp. 1901-1914, Aug. 1995.

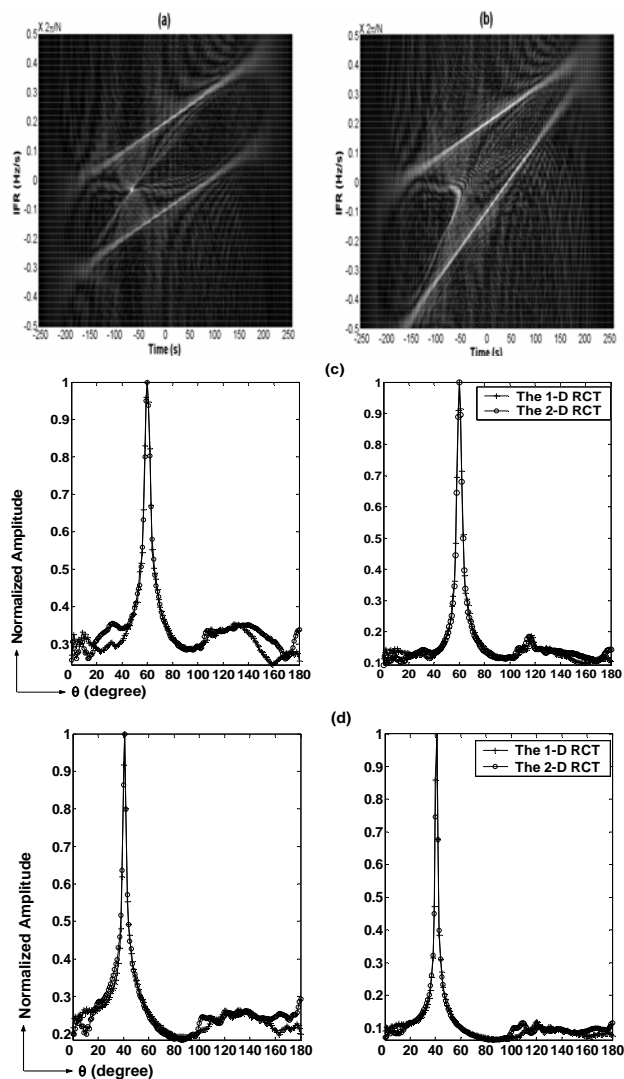


Fig.1. The identifiability problem and the results of the 1-D Radon-CPF transform. Top row — The illustration of identifiability problem; Middle row — The 1-D/2-D Radon-CPF transform over the fig.1 (a) (left: envelope estimator; right: square-law estimator); Bottom row — The 1-D/2-D Radon-CPF transform over the fig.1 (b).

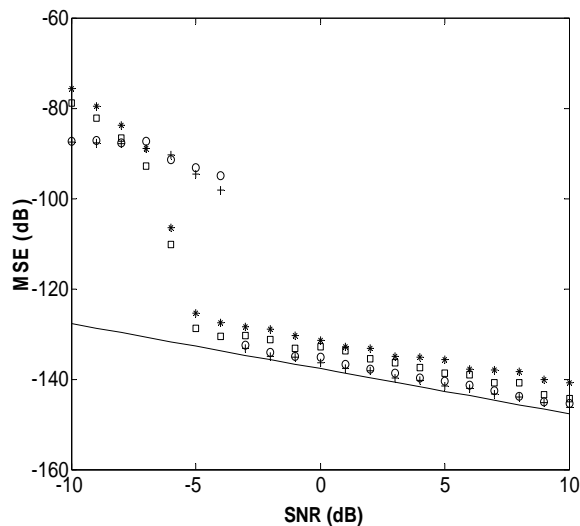


Fig.2. The MSEs of \hat{a}_3 versus SNR for 257 sample quadratic FM signal. Full line is the CRLB. Plus signs: envelope form of the 1-D Radon-CPF transform. Circles: square-law form of the 1-D Radon-CPF transform. Squares: envelope form of the 2-D Radon-CPF transform. Asterisks: square-law form of the 2-D Radon-CPF transform